Proc. Natl. Acad. Sci. USA
Vol. 95, pp. 15821–15825, December 1998
Physiology

Inositol 1,4,5-tris-phosphate activation of inositol tris-phosphate receptor Ca^{2+} channel by ligand tuning of Ca^{2+} inhibition

DON-ON DANIEL MAK*, SEAN MCBRIDE*, AND J. KEVIN FOSKETT*†‡

*Department of Physiology and †Institute for Human Gene Therapy, University of Pennsylvania, Philadelphia, PA 19104-6100

Edited by Roger Y. Tsien, University of California at San Diego, La Jolla, CA, and approved October 18, 1998 (received for review July 31, 1998)

ABSTRACT **Inositol 1,4,5-tris-phosphate (IP_3) binding to its receptors (IP_3R) in the endoplasmic reticulum (ER) activates Ca^{2+} release from the ER lumen to the cytoplasm, generating complex cytoplasmic Ca^{2+} concentration signals including temporal oscillations and propagating waves. IP_3-mediated Ca^{2+} release is also controlled by cytoplasmic Ca^{2+} concentration with both positive and negative feedback. Single-channel properties of the IP_3R in its native ER membrane were investigated by patch clamp electrophysiology of isolated *Xenopus* oocyte nuclei to determine the dependencies of IP_3R on cytoplasmic Ca^{2+} and IP_3 concentrations under rigorously defined conditions. Instead of the expected narrow bell-shaped cytoplasmic free Ca^{2+} concentration ($[Ca^{2+}]_i$) response centered at ≈300 nM–1 μM, the open probability remained elevated (≈0.8) in the presence of saturating levels (10 μM) of IP_3, even as $[Ca^{2+}]_i$ was raised to high concentrations, displaying two distinct types of functional Ca^{2+} binding sites: activating sites with half-maximal activating $[Ca^{2+}]_i$ (K_{act}) of 210 nM and Hill coefficient (H_{act}) ≈2; and inhibitory sites with half-maximal inhibitory $[Ca^{2+}]_i$ (K_{inh}) of 54 μM and Hill coefficient (H_{inh}) ≈4. Lowering IP_3 concentration was without effect on Ca^{2+} activation parameters or H_{inh}, but decreased K_{inh} with a functional half-maximal activating IP_3 concentration (K_{IP_3}) of 50 nM and Hill coefficient (H_{IP_3}) of 4 for IP_3. These results demonstrate that Ca^{2+} is a true receptor agonist, whereas the sole function of IP_3 is to relieve Ca^{2+} inhibition of IP_3R. Allosteric tuning of Ca^{2+} inhibition by IP_3 enables the individual IP_3R Ca^{2+} channel to respond in a graded fashion, which has implications for localized and global cytoplasmic Ca^{2+} concentration signaling and quantal Ca^{2+} release.**

Modulation of cytoplasmic free Ca^{2+} concentration ($[Ca^{2+}]_i$) is involved in the regulation of numerous cell physiological processes in which the second messenger inositol 1,4,5-tris-phosphate (IP_3) plays a central role in most cell types (1). Binding of extracellular ligands to G protein- or tyrosine kinase-linked receptors in the plasma membrane activates phospholipase C to generate IP_3, which binds to its receptors (IP_3R) in the endoplasmic reticulum (ER), activating them as Ca^{2+} channels to release stored Ca^{2+} from the ER lumen into the cytoplasm. The complex control of $[Ca^{2+}]_i$ is manifested temporally as repetitive spikes or oscillations (with frequencies often tuned to the level of stimulation) and spatially as propagating waves (1–3) and displays "adaptation" and "quantal release", which are poorly understood (4, 5). IP_3-mediated Ca^{2+} release is regulated by $[Ca^{2+}]_i$, with positive and negative feedback acting in a bell-shaped manner with peak Ca^{2+} release activity at ≈300 nM Ca^{2+} (6, 7); however, the mechanisms underlying this biphasic response—a fundamental component of $[Ca^{2+}]_i$ oscillations and wave propagation models (1, 3, 8)—are still poorly defined. The intracellular location of the IP_3R channel has necessitated the use of indirect measurements to infer its activity and has restricted studies of its single-channel properties (9–11). For this report, we systematically investigated the dependencies of single IP_3R channels on $[Ca^{2+}]_i$ and IP_3 concentration under rigorously defined conditions by using nuclear patch clamp of the IP_3R in its native ER membrane environment (12–15). Our results provide insights into the mechanism of channel activation by IP_3: whereas Ca^{2+} is a true receptor agonist, the sole function of IP_3 is to relieve Ca^{2+} inhibition of the channel. Ligand tuning of feedback inhibition by the permeant ion endows individual IP_3R Ca^{2+} channels with the ability to respond in a graded fashion to stimulus intensity.

METHODS

Patch clamp of the outer membrane of individual nuclei mechanically isolated from *Xenopus laevis* oocytes was performed as described (12–14). The oocyte expresses only a single IP_3R isoform (type 1) and lacks other (e.g., ryanodine receptor) Ca^{2+} release channels (16). The cytoplasmic aspect of the IP_3R channel faced into the patch pipette. All experimental solutions contained 140 mM KCl, 10 mM Hepes (pH adjusted to 7.1 with KOH), and 0 or 0.5 mM Na_2ATP as indicated. By using K^+ as the current carrier and appropriate quantities of the high-affinity Ca^{2+} chelator 1,2-bis(2-aminophenoxy)ethane-*N,N,N′,N′*-tetraacetic acid (BAPTA), the low-affinity Ca^{2+} chelator, 5,5′-dibromoBAPTA, or ATP alone to buffer Ca^{2+} in the experimental solutions, concentrations were tightly controlled in our experiments. Total Ca^{2+} content in the solutions was determined by induction-coupled plasma mass spectrometry (Mayo Medical Laboratory, Rochester, MN). Free Ca^{2+} concentrations were calculated by using the MAXCHELATOR software (C. Patton, Stanford University, Palo Alto, CA). Pipette solutions contained various concentrations of IP_3 as stated. All experiments were performed at room temperature with the pipette electrode at +20 mV relative to the reference-bath electrode. Each data point shown is the mean of results from at least four separate patch-clamp experiments performed under the same conditions. Error bars indicate the SEM. Single-channel currents were amplified by an Axopatch-1D amplifier (Axon Instruments, Foster City, CA), filtered at 1 kHz, digitized at 5 kHz, and recorded directly on hard disk by using Pulse+PulseFit 8.02 (HEKA Electronics, Lambrecht/Pfalz, Germany) on a PowerMac 8100 with an ITC-16 interface (Instrutech, Great Neck, NY). Channel dwell times and P_os were obtained by

The publication costs of this article were defrayed in part by page charge payment. This article must therefore be hereby marked "*advertisement*" in accordance with 18 U.S.C. §1734 solely to indicate this fact.

This paper was submitted directly (Track II) to the *Proceedings* office.
Abbreviations: IP_3, inositol 1,4,5-tris-phosphate; IP_3R, IP_3 receptor; $[Ca^{2+}]_i$, cytoplasmic free Ca^{2+} concentration; P_o, open probability; ER, endoplasmic reticulum; BAPTA, 1,2-bis(2-aminophenoxy)ethane-*N,N,N′,N′*-tetraacetic acid.

‡To whom reprint requests should be addressed at: Department of Physiology and Institute for Human Gene Therapy, Stellar Chance Laboratories, Room 313B/6100, University of Pennsylvania, Philadelphia, PA 19104-6100. e-mail: foskett@mail.med.upenn.edu.

using TAC 3.03 (Bruxton, Seattle, WA). Data were fitted and modeled by using IGOR PRO 3.12 (WaveMetrics, Lake Oswego, OR).

RESULTS AND DISCUSSION

$[Ca^{2+}]_i$ Dependence of the Gating of the IP_3R Channel. To examine the effects of $[Ca^{2+}]_i$ on IP_3R channel activity without possible Ca^{2+} effects on IP_3 binding, a functionally saturating IP_3 concentration of 10 μM (17) was applied to the cytoplasmic (pipette) side of the channel to fully stimulate it at various $[Ca^{2+}]_i$. With $[Ca^{2+}]_i$ corresponding to resting levels in cells (10–100 nM), the P_o of the IP_3R was low (<0.2, Fig. 1 *a* and *c*), with short open intervals ($\tau_o < 3$ ms) separated by long closed intervals ($\tau_c \approx 100$ ms; Fig. 1*b*). When $[Ca^{2+}]_i$ was increased from 100 nM to 1 μM, P_o increased dramatically to 0.8 as the result of a marked decrease of τ_c to ≈2 ms, whereas τ_o increased moderately to ≈10 ms. Similar $[Ca^{2+}]_i$ in the absence of IP_3 did not activate the channel (data not shown). Because saturating IP_3 concentrations were used, the Ca^{2+} requirement is not caused by Ca^{2+} enhancement of IP_3 affinity (18). Surprisingly, instead of the expected narrow bell-shaped $[Ca^{2+}]_i$ response centered at ≈300 nM–1 μM (9, 10, 15, 19), P_o remained very high (≈0.8) even as $[Ca^{2+}]_i$ was raised to quite high levels (1–20 μM); with long open bursts lasting >1 sec, during which the channel only closed very briefly. As $[Ca^{2+}]_i$ was increased beyond 20 μM, P_o decreased sharply, mainly the result of τ_c increasing to ≈100 ms, whereas τ_o decreased to ≈1 ms. In the presence of saturating concentrations of IP_3, there were no systematic effects on the P_o-vs.-$[Ca^{2+}]_i$ response of the species or concentration of Ca^{2+} chelator used (Fig. 1*c*), or the luminal Ca^{2+} (between 0.2 and 1.5 μM) or ATP (0 or 0.5 mM; Fig. 1*d*) concentrations.

The IP_3R P_o-vs.-$[Ca^{2+}]_i$ response in 10 μM IP_3 could be fitted to a biphasic Hill equation (Fig. 1*c*) so that:

$$P_o = P_{max}\left\{1 + \left(\frac{K_{act}}{[Ca^{2+}]_i}\right)^{H_{act}}\right\}^{-1}\left\{1 + \left(\frac{[Ca^{2+}]_i}{K_{inh}}\right)^{H_{inh}}\right\}^{-1} \quad [1]$$

This suggests that a tetrameric IP_3R channel can achieve a maximum open probability P_{max} of 0.81, with two distinct types of functional Ca^{2+} binding sites, activating sites with half-maximal activating $[Ca^{2+}]_i$, K_{act}, of 210 ± 20 nM and Hill coefficient H_{act} of 1.9 ± 0.3, and inhibitory sites with half-maximal inhibitory $[Ca^{2+}]_i$, K_{inh}, of 54 ± 3 μM and Hill coefficient H_{inh} of 3.9 ± 0.7. The large Hill coefficients, H_{act} and H_{inh}, indicate that activation and inhibition of the IP_3R by Ca^{2+} are both highly cooperative processes and suggest a requirement for Ca^{2+} binding to two of four monomers to open the channel in the presence of IP_3 and for Ca^{2+} binding to all four monomers to inhibit channel opening.

IP_3 Dependence of the $[Ca^{2+}]_i$ Sensitivity. The striking insensitivity of P_o to increases of $[Ca^{2+}]_i$ until quite high levels results in a P_o-vs.-$[Ca^{2+}]_i$ curve with a broad plateau. Previous models of complex temporal and spatial $[Ca^{2+}]_i$ signaling have assumed a much higher affinity of the inhibitory Ca^{2+} binding sites than is suggested by our data. We examined whether this discrepancy arose from our use of saturating IP_3 concentrations. However, there was no significant change in the $[Ca^{2+}]_i$ dependence when the IP_3 concentration was varied between 0.1 and 180 μM (Fig. 2). Thus, there is no evidence that the IP_3R channel possesses a low-affinity IP_3 binding site with binding coefficient >100 nM, consistent with biochemical determinations (17, 18, 20, 21). Contrary to earlier observations (22–24), no inhibitory effects of the Ca^{2+} chelator BAPTA on Ca^{2+} activation of the IP_3R were detected, even at low (20–33 nM) IP_3 concentrations (Fig. 2). At IP_3 concentrations <100 nM, however, the IP_3R became more sensitive to Ca^{2+} inhibition: at 33 nM IP_3, K_{inh} decreased to 9.5 μM, although H_{inh} and Ca^{2+} activation were not affected. Further

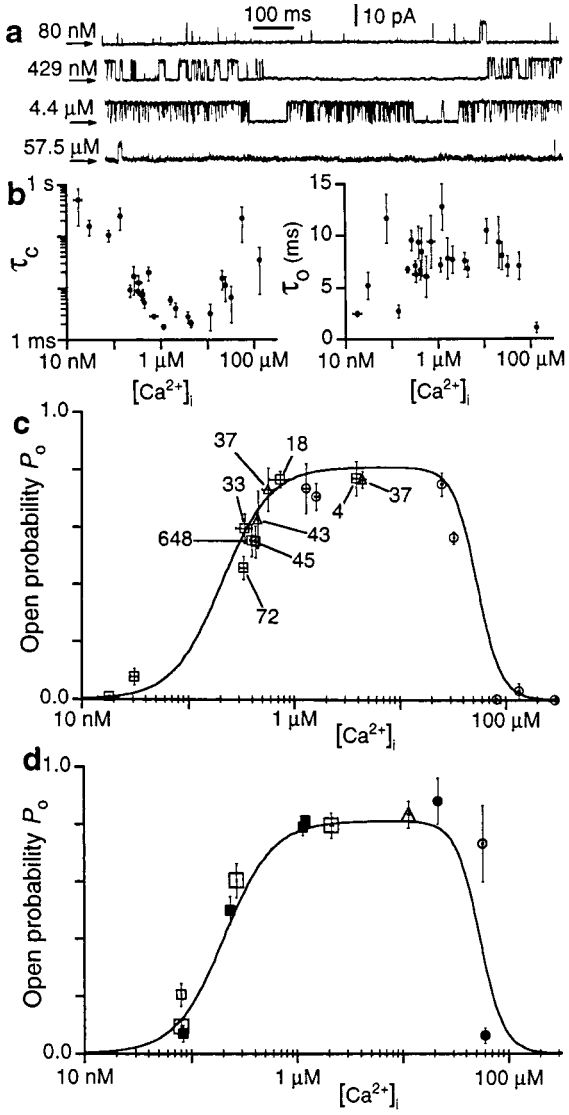

FIG. 1. $[Ca^{2+}]_i$ dependence of the IP_3R in the presence of 10 μM IP_3. (*a*) Typical single-channel current traces of the IP_3R at various $[Ca^{2+}]_i$. Arrows indicate closed-channel current level in all traces. (*b*) Dependence on $[Ca^{2+}]_i$ of mean closed-channel duration τ_c and open-channel duration τ_o of the IP_3R. (*c*) Dependence of IP_3R P_o on $[Ca^{2+}]_i$. Experiments were performed with different Ca^{2+} chelators (□, BAPTA; △, 5,5′-dibromo BAPTA, ○, ATP) in the pipette solutions. Bath solution contained 1.5 μM Ca^{2+} and 0.5 mM ATP. Numerical labels indicate calculated concentrations (in μM) of free Ca^{2+} chelators present in the pipette solutions for the corresponding data points. The solid curve is the Hill equation fit for the biphasic $[Ca^{2+}]_i$ effect on IP_3R P_o. (*d*) IP_3R P_o vs. $[Ca^{2+}]_i$ in various bath solutions. Small open symbols: 0.8 μM luminal $[Ca^{2+}]$, 0.5 mM ATP; large open symbols: 0.2 μM luminal $[Ca^{2+}]$, 0 ATP; solid symbols: 0.2 μM luminal $[Ca^{2+}]$, 0.5 mM ATP. Convention for symbols and the solid curve are the same as in *c*.

decreases in IP_3 to 10 and 20 nM caused pronounced reductions of both the maximum P_o and the range of $[Ca^{2+}]_i$ over which the IP_3R was active. The enhanced Ca^{2+} inhibition at low IP_3 concentrations cannot be explained by inhibition of IP_3 binding, because a ≈300-fold increase in $[Ca^{2+}]_i$ (from 1 to 300 μM) was required to counter the effect of only a 5-fold increase in IP_3 from 20 to 100 nM, indicating that the IP_3 relief of $[Ca^{2+}]_i$ inhibition is a highly cooperative process.

The measured P_o at all concentrations of IP_3 were fitted well by using the biphasic Hill equation (1), with K_{inh} being the only IP_3-concentration-sensitive parameter (Fig. 2). Even the observed reductions of maximum P_o and the range of $[Ca^{2+}]_i$ over

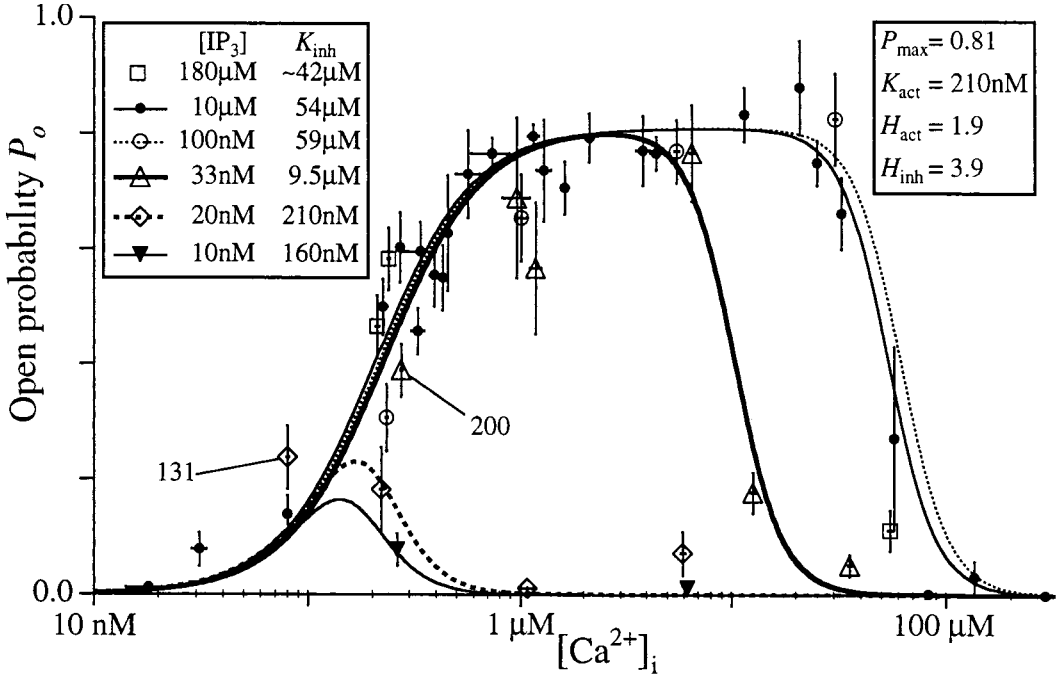

FIG. 2. IP_3-concentration dependence of the $[Ca^{2+}]_i$ sensitivity of the IP_3R. Different symbols denote data for various IP_3 concentrations as tabulated. Data points for 10 μM IP_3 were combined from experiments using various bath solutions with the same pipette $[Ca^{2+}]$. Data points for other concentrations of IP_3 were obtained in bath solutions containing 220 nM Ca^{2+} and no ATP. The curves are Hill equation fits using Eq. **1**, with K_{inh} varying with IP_3 concentration with values as listed in the graph, whereas P_{max}, K_{act}, H_{act}, and H_{inh} remained independent of IP_3 concentration, with the values tabulated in the graph. Numerical labels indicate calculated concentrations (in μM) of free Ca^{2+} chelator BAPTA present in pipette solutions used for the corresponding data points.

which the channel is active at very low IP_3 concentrations can both be accounted for in this model by a continuous decrease in K_{inh} with decreasing IP_3, whereas the other parameters: P_{max}, K_{act}, H_{act}, and H_{inh} all remain unchanged by IP_3 concentration. These data lead to an unexpected conclusion: the effect of IP_3 binding is not to enable activation of the IP_3R by Ca^{2+}, as expected for co-agonist ligands and as generally assumed (17, 18, 20, 21), but rather it is to ameliorate inhibition of the channel by Ca^{2+}. The derived values of K_{inh} ranged from 160 nM at 10 nM IP_3 to 59 μM at 100 nM IP_3. This IP_3 dependence of K_{inh} was well fitted with a simple Hill equation so that

$$K_{inh} = K_\infty \left\{ 1 + \left(\frac{K_{IP_3}}{[IP_3]} \right)^{H_{IP_3}} \right\}^{-1} \qquad [2]$$

This equation, represented in Fig. 3*a*, implies that the IP_3R has a single class of functional IP_3 binding sites with a half-maximal activating IP_3 concentration, K_{IP_3}, of 50 $\pm$ 4 nM, a Hill coefficient H_{IP_3} of 4 $\pm$ 0.5, and a maximum inhibitory Ca^{2+} binding coefficient K_∞ of 52 $\pm$ 4 μM at a saturating IP_3 concentration. The K_{IP_3} derived from this model is similar to both the dissociation constant K_D (10–100 nM) in IP_3 binding assays and IP_3 concentration required ($\approx$10–100 nM) for stimulation of Ca^{2+} release (17, 20, 21, 25). The large Hill coefficient H_{IP_3} of 4 indicates that IP_3 activation of the IP_3R is highly cooperative (25–28) even in the absence of positive feedback from cytoplasmic Ca^{2+}, requiring IP_3 binding to perhaps all four monomers of the channel to relieve the Ca^{2+} inhibition and gate the channel open. Because IP_3 binding to the IP_3R is not cooperative (17, 18, 20, 21), the similar Hill coefficients H_{IP_3} and H_{inh} (both $\approx$4) may suggest that IP_3 binding to each IP_3R monomer influences the inhibitory Ca^{2+} site in that same monomer.

According to these results, cytoplasmic Ca^{2+} at low concentrations and IP_3 both activate the IP_3R channel (Fig. 4), but they affect the channel in fundamentally different ways. Ca^{2+} binding to the IP_3R at low $[Ca^{2+}]_i$ directly activates the channel—like a conventional agonist. In contrast, IP_3 binding to the channel activates it indirectly, solely by decreasing the affinity of the Ca^{2+} inhibitory site, with no direct stimulatory effect itself. Under conditions of low IP_3 concentration, Ca^{2+} preferentially binds to the inhibitory site because of its higher affinity ($K_{inh} < K_{act}$), causing the channel to be inactive. Under conditions of stimula-

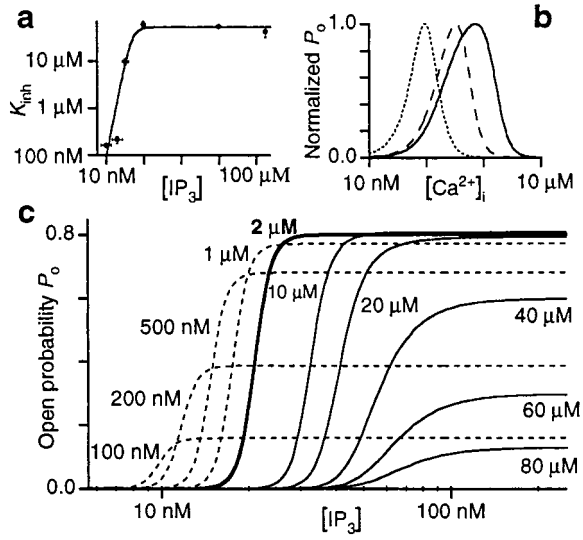

FIG. 3. (*a*) Dependence on IP_3 concentration of K_{inh} as derived from Fig. 2. The curve is a simple Hill equation fit. (*b*) Bell-shaped normalized P_o-vs.-$[Ca^{2+}]_i$ curves calculated by using Eqs. **1** and **2** for various low concentrations of IP_3 (dotted curve, 10 nM IP_3 with maximum P_o of 0.09; dashed curve, 15 nM IP_3 with maximum P_o of 0.49; and solid curve, 20 nM IP_3 with maximum P_o of 0.71). (*c*) Theoretical P_o (calculated by using the model) vs. IP_3 concentration at various $[Ca^{2+}]_i$, as labeled. Dashed curves, $[Ca^{2+}]_i \leq 1$ μM; thin solid curves, $[Ca^{2+}]_i \geq 10$ μM.

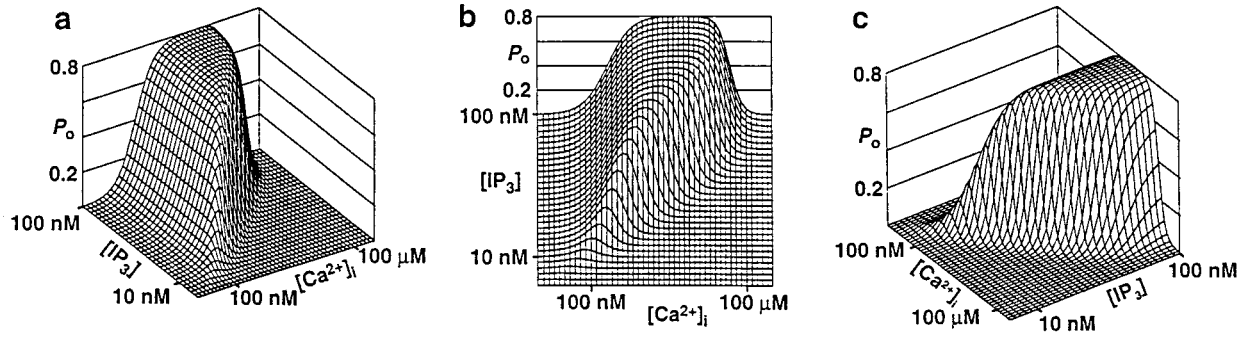

FIG. 4. Calculated P_o vs. $[Ca^{2+}]_i$ and IP_3 concentration according to our model. (*a*) Projection showing P_o-vs.-IP_3 concentration curves at various activating $[Ca^{2+}]_i$. (*b*) Projection showing P_o-vs.-$[Ca^{2+}]_i$ curves at various IP_3 concentrations. (*c*) Projection showing P_o vs. IP_3 concentration curves at various inhibitory $[Ca^{2+}]_i$.

tion associated with higher IP_3 concentration, K_{inh} becomes $>K_{act}$, so Ca^{2+} binds preferentially to the Ca^{2+} activation site, activating the channel. A recent study of reconstituted IP_3R also observed an IP_3 dependence of Ca^{2+} inhibition (11). However, the results and interpretations are fundamentally different from ours. First, the IP_3 required to observe relief from Ca^{2+} inhibition was ≈180 μM, three orders of magnitude higher than that measured here. Furthermore, P_{max} was 0.03 vs. 0.81 in our studies. Second, inhibitory effects of Ca^{2+} on the channel were not observed at 180 μM IP_3, in contrast to our results. Third, an additional low-affinity (10 μM) IP_3 binding site was invoked to account for the IP_3 relief of Ca^{2+} inhibition, whereas our data indicate that only one functional IP_3 binding site is involved, with the affinity expected (≈50 nM) from biochemical studies. Importantly, our data indicate that IP_3 mediates its effects by modulating the affinity of Ca^{2+} inhibitory sites, which is conceptually distinct from agonist activity caused by IP_3 binding to a second low affinity site.

Implications for IP_3-Mediated $[Ca^{2+}]_i$ Signaling. Our results provide another interpretation of the role of IP_3, thus warranting reconsideration of previous observations of IP_3-mediated $[Ca^{2+}]_i$ signals in cells. Our model predicts a bell-shaped relationship between P_o and $[Ca^{2+}]_i$, with a sharp peak at $[Ca^{2+}]_i$ <1 μM (9, 15, 19), although only under conditions of low (<20 nM) IP_3 (Fig. 4*b*). The low P_o and the bell shape, as well as the range of $[Ca^{2+}]_i$ over which the channel is active observed for reconstituted IP_3R channels at high (2 μM) IP_3 (9–11), are remarkably similar to the predicted channel behaviors according to our model, albeit at much lower (IP_3 ≈10 nM) concentration, suggesting an IP_3 insensitivity of the reconstituted channels in those studies. Although neither the IP_3 binding coefficient K_{IP_3} nor the Hill coefficient H_{IP_3} is $[Ca^{2+}]_i$-dependent in our model, the interplay between the effects of $[Ca^{2+}]_i$ and IP_3 concentration on P_o can be manifested as an apparent increase in IP_3 sensitivity as $[Ca^{2+}]_i$ decreases at low $[Ca^{2+}]_i$ (Fig. 3*c*) and an apparent decrease in cooperativity of IP_3 activation as $[Ca^{2+}]_i$ increases (Fig. 3*c*). Thus, our results may qualitatively explain previous observations that submicromolar $[Ca^{2+}]_i$ lowered the functional sensitivity of the IP_3R for IP_3 (29, 30) and that the Hill coefficient for IP_3 activation of Ca^{2+} release decreased as $[Ca^{2+}]_i$ increased from the submicromolar to tens of μM range (27, 28, 31).

A major paradox has been $[Ca^{2+}]_i$ responses that are graded in proportion to the intensity of the stimulus, because the process of Ca^{2+}-induced Ca^{2+} release should lead to an all-or-none signal (32, 33). One proposed mechanism suggests that increased IP_3 concentration recruits more individual elementary release units that each contribute a quantized amount of Ca^{2+} (32–35). Our model suggests another mechanism for achieving graded responses involving the IP_3R itself. Because IP_3 binding to the IP_3R relieves Ca^{2+} inhibition of the channel, higher IP_3 concentration shifts the peak of the P_o-vs.-$[Ca^{2+}]_i$ curve to higher $[Ca^{2+}]_i$ (Fig. 3*b*). A $[Ca^{2+}]_i$ that can inhibit channel activity at low IP_3 will be insufficient to inhibit it when IP_3 is increased (Fig. 4*b*). Higher $[Ca^{2+}]_i$ at the mouth of the channel pore can therefore be achieved before reaching levels that terminate release. This process therefore generates graded Ca^{2+} release from IP_3-sensitive stores through a mechanism intrinsic to the individual IP_3R. By enabling higher $[Ca^{2+}]_i$ to be achieved at the mouth of individual channels, higher IP_3 concentration associated with more intense stimuli would promote greater diffusive spread of the local $[Ca^{2+}]_i$ signal to other sites, thereby transforming highly localized signals at low levels of stimulation to more global coordinated Ca^{2+} release signals as the intensity of the stimulus is increased, without the need to invoke channels with different IP_3 sensitivities or clusters of higher channel densities (13, 32–34), although our results in no way exclude these or other mechanisms. By similar reasoning, our model can also account for the transformation of oscillating $[Ca^{2+}]_i$ at relatively low levels of agonist stimulation to sustained $[Ca^{2+}]_i$ increases during intense stimulation. Quantal Ca^{2+} release elicited by IP_3 (4, 5) has been described as a unique signaling mechanism that enables cells to retain complete responsiveness to changes in stimulus intensity (36). Our model suggests that this property can be intrinsic to the IP_3R. Because our experiments investigated the steady-state properties of the IP_3R, future kinetic studies will be required to determine the relevance of this model for quantal release in cells, as well as for other aspects of $[Ca^{2+}]_i$ signaling, including IP_3R desensitization (37) and inactivation (12, 13, 38).

We thank Dr. S. K. Joseph for reading the manuscript. This work was supported by grants from the Cystic Fibrosis Foundation and the National Institutes of Health.

1. Berridge, M. J. (1993) *Nature (London)* **361,** 315–325.
2. Meyer, T. & Stryer, L. (1991) *Annu. Rev. Biophys. Biophys. Chem.* **20,** 153–174.
3. Toescu, E. C. (1995) *Am. J. Physiol.* **269,** G173–G185.
4. Bootman, M. D. (1994) *Mol. Cell. Endocrinol.* **98,** 157–166.
5. Parys, J. B., Missiaen, L., De Smedt, H., Sienaert, I. & Casteels, R. (1996) *Pflügers Arch.* **432,** 359–367.
6. Iino, M. & Tsukioka, M. (1994) *Mol. Cell. Endocrinol.* **98,** 141–146.
7. Taylor, C. W. & Marshall, I. C. B. (1992) *Trends Biochem. Sci.* **17,** 403–407.
8. Putney, J. W., Jr., & Bird, G. S. (1993) *Endocr. Rev.* **14,** 610–631.
9. Bezprozvanny, I., Watras, J. & Ehrlich, B. E. (1991) *Nature (London)* **351,** 751–754.
10. Bezprozvanny, I. & Ehrlich, B. E. (1995) *J. Membr. Biol.* **145,** 205–216.
11. Kaftan, E. J., Ehrlich, B. E. & Watras, J. (1997) *J. Gen. Physiol.* **110,** 529–538.
12. Mak, D.-O. D. & Foskett, J. K. (1994) *J. Biol. Chem.* **269,** 29375–29378.

13. Mak, D.-O. D. & Foskett, J. K. (1997) *J. Gen. Physiol.* **109,** 571–587.
14. Mak, D.-O. D & Foskett, J. K. (1998) *Am. J. Physiol.* **275,** C179–C188.
15. Stehno-Bittel, L., Lückhoff, A. & Clapham, D. E. (1995) *Neuron* **14,** 163–167.
16. Kume, S., Muto, A., Aruga, J., Nakagawa, T., Michikawa, T., Furuichi, T., Nakade, S., Okano, H. & Mikoshiba, K. (1993) *Cell* **73,** 555–570.
17. Mauger, J.-P., Lièvremont, J.-P., Piétri-Rouxel, F., Hilly, M. & Coquil, J.-F. (1994) *Mol. Cell. Endocrinol.* **98,** 133–139.
18. Taylor, C. W. & Traynor, D. (1995) *J. Membr. Biol.* **145,** 109–118.
19. Iino, M. (1990) *J. Gen. Physiol.* **95,** 1103–1122.
20. Taylor, C. W. & Richardson, A. (1991) *Pharmacol. Ther.* **51,** 97–137.
21. Joseph, S. K. (1995) *Cell. Signalling* **8,** 1–7.
22. Richardson, A. & Taylor, C. W. (1993) *J. Biol. Chem.* **268,** 11528–11533.
23. Combettes, L. & Champeil, P. (1994) *Science* **265,** 813.
24. Combettes, L., Hannaert-Merah, Z., Coquil, J.-F., Rousseau, C., Claret, M., Swillens, S. & Champeil, P. (1994) *J. Biol. Chem.* **269,** 17561–17571.
25. Meyer, T., Holowka, D. & Stryer, L. (1988) *Science* **240,** 653–655.
26. Carter, T. D. & Ogden, D. (1997) *J. Physiol. (Lond.)* **504,** 17–33.
27. Finch, E. A., Turner, T. J. & Goldin, S. M. (1991) *Science* **252,** 443–446.
28. Dufour, J. F., Arias, I. M. & Turner, T. J. (1997) *J. Biol. Chem.* **272,** 2675–2681.
29. Hirose, K., Kadowaki, S. & Iino, M. (1998) *J. Physiol. (Lond.)* **506,** 407–414.
30. Missiaen, L., De Smedt, H., Droogmans, G. & Casteels, R. (1992) *J. Biol. Chem.* **267,** 22961–22966.
31. Combettes, L., Claret, M. & Champeil, P. (1992) *FEBS Lett.* **301,** 287–290.
32. Bootman, M. D. & Berridge, M. J. (1995) *Cell* **83,** 675–678.
33. Berridge, M. J. (1997) *J. Physiol. (Lond.)* **499,** 291–306.
34. Horne, J. H. & Meyer, T. (1997) *Science* **276,** 1690–1693.
35. Callamaras, N., Marchant, J. S., Sun, X. P. & Parker, I. (1998) *J. Physiol. (Lond.)* **509,** 81–91.
36. Kindman, L. A. & Meyer, T. (1993) *Biochemistry* **32,** 1270–1277.
37. Oancea, E. & Meyer, T. (1996) *J. Biol. Chem.* **271,** 17253–17260.
38. Hajnóczky, G. & Thomas, A. P. (1994) *Nature (London)* **370,** 474–477.